AIAA SciTech Forum
9 - 13 January 2017, Grapevine, Texas
55th AIAA Aerospace Sciences Meeting

Critical Mach Number Prediction on Swept Wings

Jeffrey J. Kirkman[1]
and
Timothy T. Takahashi[2]

Arizona State University, Tempe, AZ, 85287-6106

Busemann's famous swept wing theory forever changed the shape of aircraft and air travel. Since 1935, aircraft engineers have been employing sweep to delay the onset of drag rise. While "simple sweep theory" has been widely accepted as truth, this work uncovers certain inconsistencies that limit its general utility. We show here that the consensus understanding of Busemann's theory is only accurate for qualitative trend prediction. Indeed, Küchemann correctly described an exact prediction method to estimate the critical Mach number of flow over real swept wings. In this work, we explain the reason for the discrepancy between Busemann's simple sweep theory and Küchemann's more refined model.

I. Introduction

IN the modern era of, speed and efficiency are vital aspects driving the overall design of aircraft. Society expects new aircraft to fly faster, further, and cheaper than their predecessors do. As Gabrielli & Karman famously noted, it is not merely mechanical efficiency but the product of mechanical efficiency and speed that governs the transportation system efficiency [1]. One approach to increasing speed, without a loss of mechanical efficiency is to incorporate leading edge sweep into the design of aircraft.

Adolf Busemann in a paper given at the 1935 Volta Congress meeting, [2, 3] was the first to postulate the use of sweep to delay the onset of transonic drag rise. During the Second World War, his ideas were qualitatively confirmed by Ludwieg [4] and Ackeret [5]. However, these ideas did not influence aerodynamic design in the United States until after the war when R.T. Jones became its most prominent evangelist [6]. While wing sweep has transformed aircraft design, its underlying physical explanation has suffered from inconsistent explanation.

Within our own research group, in work presented at the 2014 AIAA AVIATION conference, Takahashi, Dulin & Kady found inconsistencies in implications arising from the consensus understanding of Busemann's Simple Sweep Theory [7]. In a continuation of this work, presented in 2015 AIAA AVIATION conference, Takahashi & Kamat employed modern CFD to document the sources of these inconsistencies [8]. While making some progress on better explaining the potential flow mechanisms behind sweep theory, they found evidence that the published methods that predict the critical Mach number were inadequate. Work presented by the current authors, Kirkman & Takahashi, at the 2016 AIAA Aviation conference shows inconsistencies with the Transonic Similarity Rule and the fundamental inconsistencies between the Critical Pressure Coefficient equations [9].

In this work we set forth to conclude our research. Here, we document the appropriate predictive equation to estimate the critical pressure coefficient on a swept wing. It differs in minor, but critically important ways, from many other published references.

[1] M.S. Candidate Aerospace and Mechanical Engineering, School for Engineering of Matter, Transport & Energy, P.O. Box 876106, Tempe, AZ. Student Member AIAA.
[2] Professor of Practice, Aerospace and Mechanical Engineering, School for Engineering of Matter, Transport & Energy, P.O. Box 876106, Tempe, AZ. Associate Fellow AIAA.

II. Prior Art

Simple, quantitative means to predict for shock formation on a swept wing remains troublingly inconsistent ever since Adolf Busemann gave his famous paper at the 1935 Volta Congress [2]. Many authors [10,11,12,13,14] reproduce the original figures and data sets collected by Busemann and his collaborators at Göttingen. Typically, they conceptually explain how sweep delays the onset of compressibility effects on the wing, but refrain from calculating the actual Critical Mach Number, and therefore the Critical Pressure Coefficient relationship that governs swept and sheared wings.

A. Adolf Busemann – Sweep Theory

Busemann's early work [2] demonstrated that a swept wing delays the onset of drag rise. He argued that sweep decreases the Mach number of the flow normal to the leading edge of the wing, therefore the Mach dependent compressibility effects follow the leading edge Mach number.

Busemann [2,3] postulated that a swept wing, of angle φ, acts like an infinite span wing yawed at angle φ to the wind. This indicates that the two-dimensional airfoil section is defined normal to the leading edge instead of a "sheared" wing where the aerodynamicist defines the airfoil section in the wind axis (see Figure 1).

Busemann claimed that the flow normal to the leading edge is the crucial component. In his argument, the spanwise flow has no major impact on the critical flight conditions.

This assumption has been a widely accepted and is the basis for sweep theory. In our work, we will demonstrate that this simplification renders his theory inexact.

B. Hubert Ludwieg – Testing Swept Wings

In 1939, four years after Busemann first presented his work on swept wings, Hubert Ludwieg began preparations for tests in the newly operational supersonic wind tunnel in Göttingen [3]. Ludwieg, deputized by Albert Betz, built two models of the same airfoil section, but with different sweep angles. The first was a trapezoidal wing without sweep, and the second a trapezoidal wing with 45 degrees of sweep (see Figure 2). His work utilized a relatively thick, low-speed airfoil in order to ensure the improvements of sweep postulated by Busemann were easily visible at reasonable Mach numbers.

We reproduce the results of Ludwieg's testing as Figure 3 [4]. Here, we can see that the swept wing does provide advantage in the higher subsonic regime. This data is taken at $M_\infty = 0.7$ and $M_\infty = 0.9$ with the most notable advantages being seen in the Lift vs. Drag curves. In the straight wing data, there is an obvious increase in drag, that is not present in the swept wing data. This data qualitatively confirms Busemann's insight.

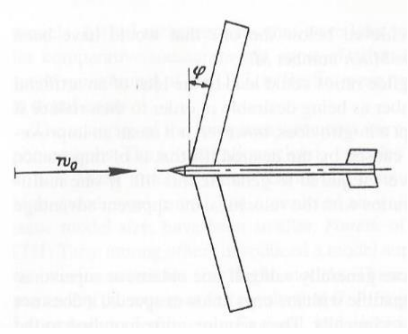

Figure 1. Busemann's original sketch of the swept wing.

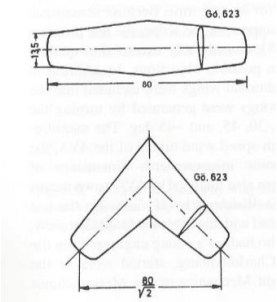

Figure 2. Ludwieg's sketch of the original test wings.

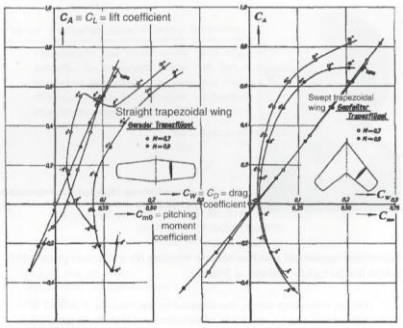

Figure 3. Ludwieg's data from his first swept wing tests.

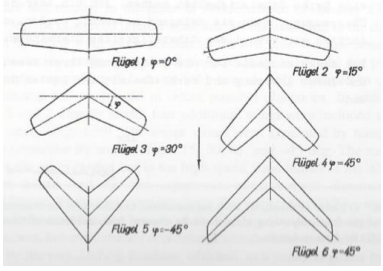

Figure 4. Ludwieg's wings for the expansion of the test program

Due to many skeptics to the test program, Ludwieg further expanded these tests [3]. Figure 4 shows the expansion of the test wings for the second round of testing [15]. These tests featured wings with various sweep angles, including one with forward (negative) sweep. Since Busemann's theory postulated that the Mach number normal to the leading edge was the driving factor, there should be no difference between a forward swept wing or a swept back wing, in terms of delaying the drag divergence.

Once again, Ludwieg found that the effects of sweep postulated by Busemann were qualitatively correct. In Figure 5, we see that the drag coefficient decreases with increasing sweep angle for the flow at $M = 0.8$. Ludwieg also found that the forward swept wing had almost the same aerodynamic qualities of the swept back wing. The reader should understand that these findings only prove that Busemann was qualitatively correct; they do not provide the full story.

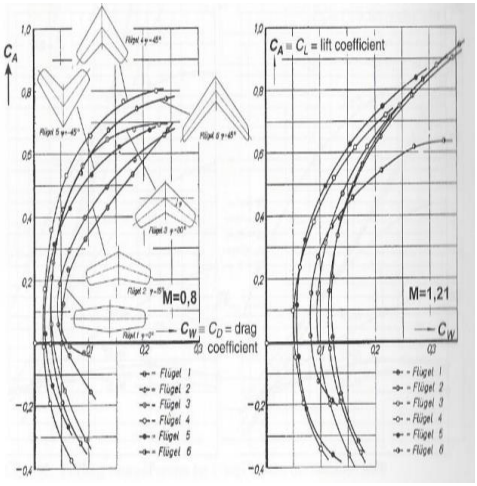

Figure 5. Ludwieg's results from the second round of testing.

C. Jakob Ackeret – Testing Swept Wings

Jakob Ackeret addressed wing sweep briefly in NACA TM 1320 [16]. In this report, Ackeret discusses the wind tunnel set up and corrections done in order to test four different sections. The four sections are: 1) unswept 12% thick wing, 2) unswept 9% thick wing, 3) 12% thickness section with 35 degrees sweep, and 4) 9 % thickness section with 35 degrees sweep. Figure 6 shows the results from Ackeret's work.

Ackeret[16] did not provide an analytical explanation to the sweep correction. Instead, he developed an empirical fit to the collected experimental data. On one hand, he stated that his data followed Kármán's Similarity Rule (the idea that flow over a wing at high Mach numbers is functionally equivalent to the low speed, potential flow, over a wing with transformed geometry). On the other hand, he fitted a 3/2 power to the acquired data (a fitting function which is completely unrelated to any explanations given be Kármán's Similarity Rule).

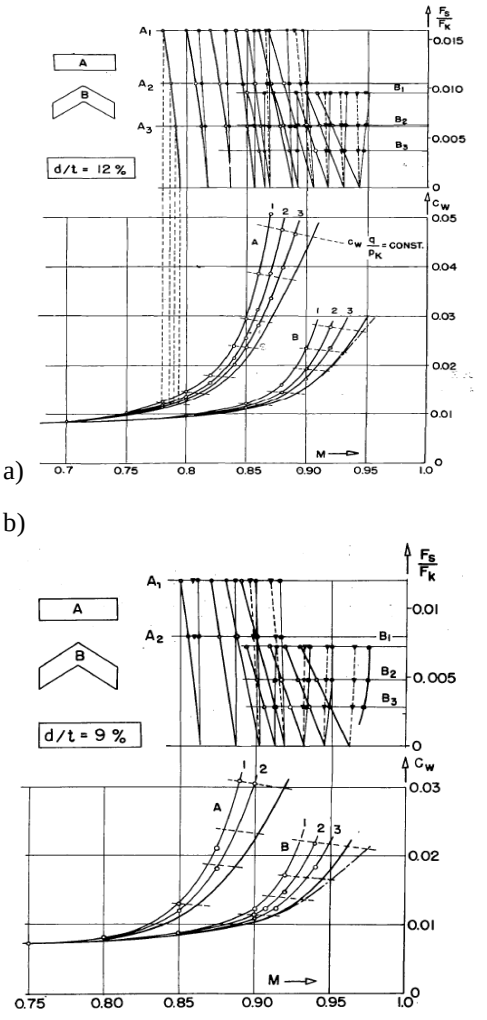

Figure 6. Ackeret test data on a) 12% wing sections and b) 9% wing sections.

D. R.T. Jones – Classical Simple Sweep Theory

RT Jones cited back to Busemann [2,3] and Betz [17] (Ludwieg worked for Betz) in his work on *High Speed Wing Theory* [6,10]. In his writing, Jones further explains how the swept wing geometry affects the flow. He argues that the pressure forces on the wing will act normal to its axis and therefore both the pressure drag and the lift should be reduced by a factor proportional to $(\cos\varphi)^2$. Jones places a broad transformation here into how the swept wing affects the lift and drag, compared to a straight wing.

Jones' derivation follows Busemann's original postulate regarding flows around swept wings. Recall that Busemann stated that only the flow normal to the leading edge of the wing is important in determining the flow properties over a swept wing; we can neglect all contributions that arise from the implied spanwise flow. Jones' argument holds that the effective velocity

over the wing is decreased by the cosine of the sweep angle. This assumption leads to Jones' transformation to the pressure coefficient, the dynamic pressure, the lift the lift curve slope, yet a single cosine on the lift coefficient.

Equations 1 through 3 show the transformations Jones' makes on the incompressible unswept data to the compressible data for the swept wing.

$$\frac{\Delta p}{\frac{1}{2}\rho U^2} = \frac{f(\xi)}{\sqrt{1-(M_\infty \cos\varphi)^2}} \tag{1}$$

$$C_L = \frac{2\pi\alpha\cos\varphi}{\sqrt{1-(M_\infty \cos\varphi)^2}} \tag{2}$$

$$\left(\frac{\delta C_L}{\delta\alpha}\right)_{M_\infty,\varphi} = \left(\frac{\delta C_L}{\delta\alpha}\right)_{0,0} \frac{(cos\varphi)^2}{\sqrt{1-(M_\infty \cos\varphi)^2}} \tag{3}$$

It is these transformations that Takahashi, Dulin & Kady set out to correlate to finite swept wing data.

E. Takahashi, Dulin & Kady – Revisiting RT Jones

The trio of Takahashi, Dulin & Kady [7] employed potential flow solvers to determine the pressure coefficient across swept wings and to correlate the data from Busemann's work to the explanation from R.T. Jones. Their work focused entirely on interrogating the results of a finite swept wing as modelled by a potential flow solver [18]. They modelled pure thin wings (with no thickness) as well as practical wings (with finite thickness). They collected overall lift, net (upper-lower) and specific surface pressures. However, this solver, while employing a compressibility correction does not capture the formation of shock waves.

In their new work, Takahashi, Dulin & Kady found that there were some inconsistencies between Jones and Busemann. They discovered that actual lift and surface pressure data did not follow the cosine squared transformation as implied by R.T. Jones' literal explanation of Busemann's theory. Indeed, they found that their data fits seemed to indicate that a cosine transformation (as opposed to cosine squared) better explains real world finite swept wing data.

Equation 4 shows their proposed transformation on the pressure coefficient. Due to the flow transformation, and a geometric transformation, Takahashi, Dulin & Kady proposed that the swept wing transformation is a single cosine.

$$Cp'\left(\frac{x}{c_{LE}}\right) = \frac{Cp_{wind}\left(\frac{x}{c_{LE}}\right)}{\cos(\varphi)} = \frac{\Delta P}{\frac{1}{2}\rho(U_\infty cos\varphi)^2}\cos(\varphi) \tag{4}$$

F. Takahashi & Kamat – Revisiting Busemann

Takahashi & Kamat [8] set to validate Busemann's findings for infinitely swept wings, determine the correction for sheared wings, and further test the findings of Takahashi, Dulin, & Kady. This work employed modern CFD methods to validate the results of the potential flow solvers and determine the correct sweep transformation.

Takahashi & Kamat found that the sheared wing data does not collapse to the explanation given by Busemann. They also find that the cosine correction given by Takahashi, Dulin & Kady did not quite fit the data either. That is, for subcritical flows, the single cosine transformation seemed to explain changes in lift slope quite well. But neither the single cosine nor the cosine squared transformation, when applied to the critical pressure equation seemed to predict shock formation with any degree of accuracy.

G. Takahashi and Kirkman – Study of Applicability of Famous 2D Critical Pressure Equations

The current authors presented work at AIAA AVIATION 2016, in which they examined the basic two dimensional critical pressure coefficient equations [9]. This work used ANSYS Fluent to determine the critical condition over two dimensional airfoils.

We began with the critical pressure derivations of Hermann Schlichting, Dietrich Küchemann, Theodore Von Kármán, John Anderson, and Eastman Jacobs. The equations of Küchemann, Anderson, and Eastman Jacobs were all derived through thermodynamic relationships and found to be mathematically equivalent. Both Von Karmn and Schlichting derived their critical pressure coefficients through linear approximations. Equations 5 through 8 show the various famous equations for the critical pressure coefficient.

Schlichting:

$$Cp^* = -\frac{2}{\gamma+1}\frac{1-Ma_{\infty_{cr}}^2}{Ma_{\infty_{cr}}^2} \tag{5}$$

Küchemann:

$$Cp^* = \frac{2}{\gamma M_\infty^2}\left\{\left(\frac{2}{\gamma+1}\right)^{\frac{\gamma}{\gamma-1}}\left(1+\frac{\gamma-1}{2}M_\infty^2\right)^{\frac{\gamma}{\gamma-1}}-1\right\} \tag{6}$$

Eastman Jacobs and Anderson:

$$Cp^* = -\frac{2}{\gamma M_\infty^2}\left\{\left[\frac{2+(\gamma-1)M_\infty^2}{\gamma+1}\right]^{\gamma/(\gamma-1)}-1\right\} \tag{7}$$

Von Kármán

$$Cp^* = \frac{2\left[\left(1-M_\infty^2\right)^{3/2}\cdot\left(1+M_\infty^2\right)^{1/2}\right]}{M_\infty} \tag{8}$$

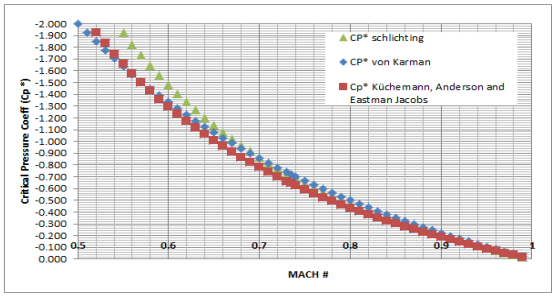

Figure 7- Comparison of *Cp** equations (Schilchting, von Kármán, Küchemann, E. Jacobs and Anderson. *Cp** as a function of Mach.

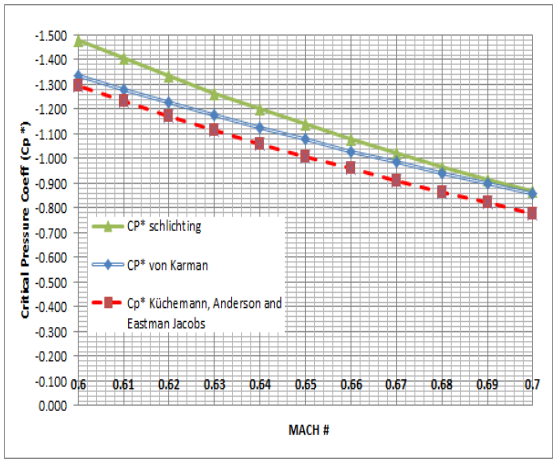

Figure 8- Detailed comparison of *Cp** equations (Schlichting, von Kármán, Küchemann, E. Jacobs and Anderson. *Cp** as a function of Mach at a typical airfoil design point.

We plot these equations as of function of Mach number in Figures 7 and 8, reproduced from Takahashi and Kirkman AIAA AVIATION 2016 paper [9]. These figures show the difference in two dimensions between the various equations, and it was this difference that the current authors set to differentiate.

The results found that the thermodynamic derivations of Küchemann, Eastman Jacobs and Anderson correctly predicted the critical condition on the airfoil. These findings were crucial in this work to determine the correct pressure coefficient equation for a swept wing.

H. Hermann Schlichting – Swept Wing Critical Pressure Equation

Schlichting [14] approached the critical pressure coefficient for a sweptback wing of constant chord and infinite span. He argued that the critical condition is dependent upon the flow normal to the leading edge of the wing. This led to his derivation of the critical pressure coefficient for a swept wing :

$$Cp^* = -\frac{2}{\gamma+1}\frac{1-Ma_{\infty_{cr}}^2(\cos\varphi)^2}{Ma_{\infty_{cr}}^2} \tag{9}$$

The sweep angle enters the numerator of this equation here. It is interesting that he derives a function where the critical conditions is governed by both the Mach number of the flow normal to the leading edge and the freestream Mach number.

I. Dietrich Küchemann – Swept Wing Critical Pressure Equation

Küchemann's equation estimates the critical pressure coefficient for a swept wing.

$$Cp^* = \frac{2}{\gamma M_\infty^2}\left\{\left(\frac{2}{\gamma+1}\right)^{\frac{\gamma}{\gamma-1}}\left(1+\frac{\gamma-1}{2}M_\infty^2\,(\cos\varphi)^2\right)^{\frac{\gamma}{\gamma-1}}-1\right\} \tag{10}$$

Küchemann derived this equation through the thermodynamic relationships between the static pressure and total head and the local velocity and the sweep of the isobars. In equation 10 the freestream Mach number is found in the numerator and denominator (as seen in the various equations) yet only applies a sweep transformation to the numerator. The denominator remains dependent upon the freestream Mach number, without the sweep transformation, similar to Schlichting. Unlike Busemann or Jones, this method captures elements of the magnitude of the freestream as well as the leading-edge flow.

Küchemann's [12] sweep transformation is based upon his equation for the local velocity of sound. Shown here in equation 11, Küchemann states that the local sonic velocity is based upon the sweep of the isobars (and therefore the sweep of the wing).

$$\left(\frac{V}{V_0}\right)^* = \{1+\frac{2}{(\gamma+1)M_\infty^2}(1-M_\infty^2\,(\cos\varphi)^2\}^{\frac{1}{2}} \tag{11}$$

This equation shows that the sonic conditions of the flow are dependent upon the freestream flow Mach number and the sweep angle of the wing.

J. Stefan Neumark – Technique for Correction between unswept and swept wing properties

In 1949, Stefan Neumark published work on Critical Mach predictions for swept wings [19]. He derived the Critical Mach number for straight untampered wings and then adds his correction of $\cos\varphi$ to each Mach number in the equation, therefore indicating the Critical condition is only dependent upon the Mach number normal to the leading edge.

This differs from Küchemann's and Schlichting's derivation, where the critical condition is defined not only by the Mach number normal to the leading edge, but also the freestream Mach number. This research refers to Neumark's proposed modification in determining the Critical Mach Number, and therefore the Critical Pressure Coefficient, as the "Neumark Modification".

The "Neumark Modification" implies that the sweep corrections should be applied to each Mach number term to the pressure coefficient equation. Equation 12 shows the implied transformation.

$$Cp(M) = Cp(M*\cos\varphi) \tag{12}$$

This differs from Küchemann and Schlichting's derivations of the critical Pressure coefficient. Both authors derived the Pressure Coefficient for a swept wing aircraft, and they both agree that the transformation only occurs to the Mach number in the numerator. This is a major difference that creates the variation in the Critical Pressure Coefficient for a swept wing.

For study, we may apply Neumark's correction to several famous 2D critical pressure coefficient equations.

For example, Anderson's [11] equation for the Critical Pressure Coefficient, $Cp^* = -\frac{2}{\gamma M_\infty^2}\left\{\left[\frac{2+(\gamma-1)M_\infty^2}{\gamma+1}\right]^{\gamma/(\gamma-1)}-1\right\}$ does not have a sweep correction. In our present work, we equation was modified with the "Neumark Modification" in order to properly transform it into the correct axis frame. In Equation 13, we present Anderson's equation incorporating the "Neumark Modification" for swept wings.

$$Cp^* = -\frac{2}{\gamma M_\infty^2 (\cos\varphi)^2}\left\{\left[\frac{2+(\gamma-1)M_\infty^2(\cos\varphi)^2}{\gamma+1}\right]^{\gamma/(\gamma-1)} - 1\right\} \quad (13)$$

In this equation, we apply the sweep correction to the numerator and denominator, per Neumark. With this sweep correction, the equation is equivalent to the Eastman Jacobs derivation [20] with the "Neumark Modification".

Eastman Jacobs' derivation is based upon thermodynamic relationships. The fundamental work does not consider its applicability to swept wings. His equation for critical Mach number is functionally identical to equation 7, but with some algebraic shuffling of terms. In Figure 14, we present Eastman Jacobs' equation incorporating the "Neumark Modification" for swept wings:

$$Cp^* = \frac{2\left[1-\left(\frac{2+(\gamma-1)M_\infty^2(\cos\varphi)^2}{\gamma+1}\right)^{\gamma/(\gamma-1)}\right]}{\gamma M_\infty^2(\cos\varphi)^2} \quad (14)$$

This equation has the sweep correction in the numerator and the denominator. Unlike the equations for no sweep, this equation differs from Küchemann. However, this equation is still mathematically equivalent to Anderson's equation with the Neumark Modification.

Von Kármán does not address sweep in his derivation of the critical pressure coefficient in his work dating from 1941[20]. Although it was following the Volta Congress, it predates R.T Jones' work in the United States.

In order to apply Von Kármán's equation to sweep the "Neumark Modification" was used in this research (equation 15).

$$Cp^* = \frac{2\left[\left(1-M_\infty^2(\cos\varphi)^2\right)^{3/2}\cdot\left(1+M_\infty^2(\cos\varphi)^2\right)^{1/2}\right]}{M_\infty\cos\varphi} \quad (15)$$

K. Bertin & Cummings – Description of Sweep Effects

Bertin & Cummings [13] addressed swept wings all too briefly in their book Aerodynamics for Engineers. The pair reproduced the data from the original swept wing testing and only discussed the effects of sweep. There is no discussion in designing an aircraft for specified sweep or on the predictors to shock formation on the swept wing.

L. McLean – Description of Sweep Effects

McLean address wing sweep in his book Understanding Aerodynamics [21]. In his discussion of the swept wing, McLean states that the critical conditions are dependent upon the Mach number perpendicular to the isobars of the wing. Although the isobars should more or less follow the sweep of the wing, this is not always the case and is a distinction from the sweep corrections of various authors.

McLean [21] states that the pressure coefficient of the three-dimensional wing is the two-dimensional data transformed by $(\cos\varphi)^2$.

$$Cp_{3D} = Cp_{2D}(\cos\varphi)^2 \quad (16)$$

This equation by McLean argues that the transformation to the pressure coefficient is the $(\cos\varphi)^2$ but doesn't explain how it is applied. Neumark applies his transformation to the flow normal to the leading edge of the swept wing. McLean suggests that the transformation to the pressure coefficient is a broad application.

III. PROBLEM FORMULATION

To understand the practical differences between the various Critical Pressure Coefficient equations, each equation was plotted as a function of Mach number and for 40 degrees of sweep. As can be seen in Figure 9, each equation differs significantly between one another. Between these equations, a wing with 40 degrees of sweep, and a minimum pressure coefficient of -1, has a Critical Mach Number range of ~0.72 to ~ 0.84. This is a large discrepancy that could mean the difference in making or missing cruise and performance guarantees for an aircraft. It is this discrepancy that this work set to sort out.

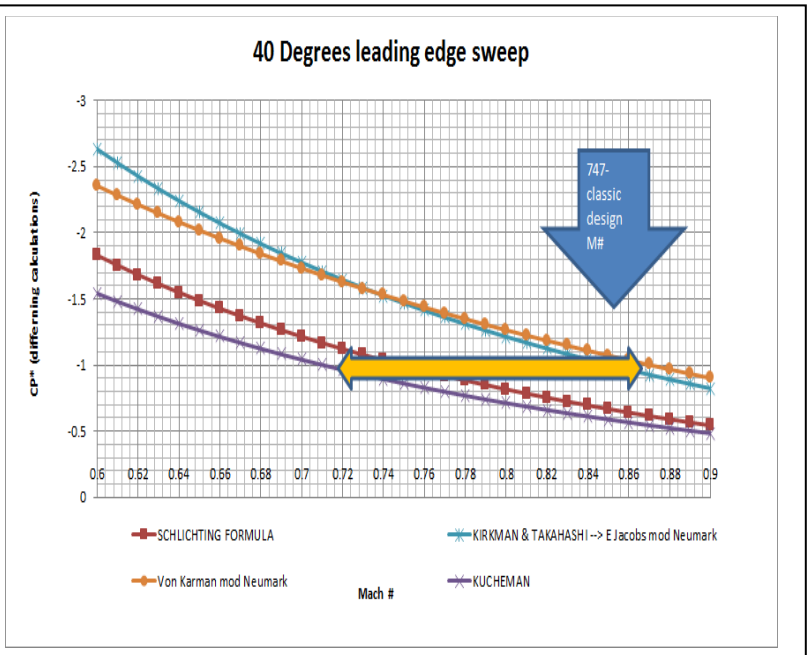

Figure 9. Critical Pressure Coefficient equations for 40 degrees of sweep.

To further understand how the sweep theory applies to gas dynamics, the current authors turned to the theory of oblique shocks. Although there are some consistencies across authors, many authors do not agree in the explanation in the formation of the oblique shock.

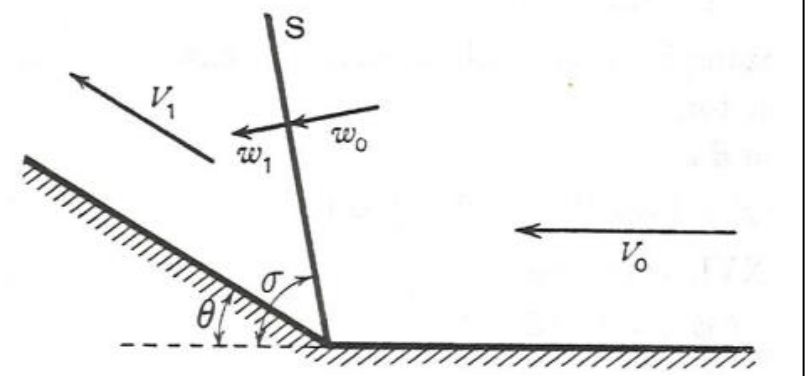

Figure 10. Oblique shock diagram. [23]

In NACA 1135 the formation of the oblique shock is described as a normal shock to the component of flow perpendicular to the shock wave (Figure 10) [22]. This description lends itself to the sweep principles of Busemann and Jones, where the flow normal to the leading edge (or in this case the shock wave) is important. An interesting point made in NACA 1135 is that the strength of the shock wave is determined from the flow perpendicular to the oblique shock, yet the tangential flow still influences the speed of sound. This important relationship is where further derivations of the oblique shock relationships are found.

In this work, we perform necessary computations through legacy open-source aerodynamic codes as well as using commercial computational fluid dynamics (CFD). These computations included running various wings and airfoils at various Mach numbers and angles of attack. The purpose was to gather data to clarify the mysterious phenomena of "stretching" and to determine the "most correct" equation for the Critical Pressure Coefficient of both and unswept, and swept section.

A. VORLAX

VORLAX is a compressibility-corrected subsonic/supersonic potential flow solver developed by Lockheed-California (now Lockheed Martin) under contract from NASA [18]. The code allows the user to input geometry in

three forms: 1) simple, thin flat panels, 2) thin, cambered panels, or 3) a thickness simulating "sandwich panels." [18] VORLAX outputs a variety of flow solution data: 1) overall force and moment coefficients suitable to build an aerodynamic database (lift, drag, side force, pitching moment, rolling moment, and yawing moment), 2) surface panel net differential pressure coefficients (for thin flat and cambered panels), 3) surface panel actual pressure coefficients (for thickness simulated "sandwich panels), and 4) off-body wake survey velocity vectors. VORLAX was used to determine the correct forms of the various transformations proposed by Schlichting. VORLAX is also used alongside CFD to investigate Critical Mach Number predictive capabilities of the various equations. Because VORLAX is incapable of simulating a shock wave, it can only identify regions of incipient sonic flow where the VORLAX solution will diverge significantly from both reality and a CFD solution.

B. ANSYS Fluent

ANSYS Fluent software solves the Navier-Stokes equations through either a density-based or pressure-based solver [24]. Due to the analysis of airfoils being in the transonic regime, the density-based solver was used.

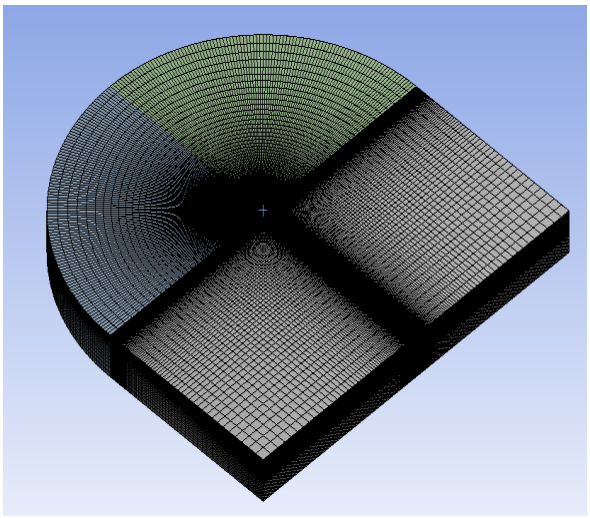

Figure 11. Isometric view of the three-dimensional c-grid.

In the density based solver of ANSYS, the flow properties are calculated simultaneously. This differs from the pressure based solver, where each of the flow properties are solved individually. The other difference between these equations is the derivation of the governing equations. The pressure based solver derives the continuity equation with the velocity field, where as the density based solver is based upon the continuity, momentum, and energy equations. For transonic flow and shock waves, the governing equations to the density based solver are preferred.

The initial CFD runs were performed using a three-dimensional C-grid with the inlet and outlet placed a large distance from the airfoil in order to prevent interference of the boundaries with the solution with a periodic boundary on the left and right walls. These runs were done with the transient solution option in ANSYS Fluent. Figure 11 shows the initial three dimensional grid used to calculate the pressure across the airfoil.

In calculating the transient solution, a new source of error occurs. In order to calculate an accurate solution, the grid must be refined not only in the step size but also the time step. These solutions were iterated until steady-state, defined where the data over multiple time steps did not vary, was achieved in the flow. The transient setup allowed much finer grids to converge to a stable solution when compared with the steady-state option in ANSYS Fluent.

The grid was setup normal to the leading edge of a "sheared" wing. This means that the actual airfoil tested is a transformed version of the NACA 64-012 airfoil tested.

Figure 12 shows the sweep transformation on the airfoil. In this image the original airfoil is shown as the sketched spline. This airfoil is defined in the wind axis of the wing. The cutout in the figure below shows the airfoil defined off the leading edge of the swept wing. In this figure it can be seen that the thickness form does not change due to sweep, however the airfoil chord is transformed by the cosine of the sweep.

To define the flow velocities in the solution reference frame, the freestream velocities had to be transformed. The coordinate system transformations are shown as equations 17a through 17d. The coordinate system being defined as 1) x is the chord wise direction normal to the leading edge, 2) y is the spanwise direction, and 3) z is the vertical direction, with positive z pointing towards the upper surface of the airfoil.

$$V_x = V\cos\varphi\cos\alpha \quad (17a)$$
$$V_y = V\sin\varphi\cos\alpha \quad (17b)$$
$$V_z = V\sin\alpha \quad (17c)$$

Where:

$$V = M * a \quad (17d)$$

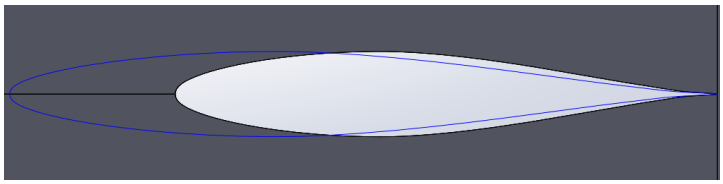

Figure 12. Swept airfoil geometry.

These equations depend upon both the angle of attack, α, and the sweep angle, φ.

Due to the geometry effects of the sweep angle on the grid, we varied only the angle of attack and Mach number for each grid setup. For this work, we only considered solutions representing 40 degrees sweep; this maximizes the variance between the various candidate Critical Pressure Coefficient equations.

We checked the accuracy of the solutions by a grid refinement by decreasing the step size, *h*, by a factor of 1.34 from the original grid, and a second time to the modified grid. This process provided three distinct solutions of the same flight condition, each with a finer grid than the previous. Using a Grid Convergence Index, the accuracy of the coarsest grid can be determined. We repeated this process for each new grid tested. Since this testing is only done on the actual grid size, it is acceptable to use the same grid across the flight conditions with great confidence.

IV. Trade Studies

As discussed in Prior Art section, there are many takes on the necessary correction for estimating the Critical Pressure Coefficient on a swept wing. The final goal of this research is to determine which correction factor accurately predicts the critical conditions across a swept section or, if none of the current methods are found to be correct, determine a correction based upon the sweep of the section.

Returning to Figure 9 (page 8), the four Critical Pressure Coefficient equations with 40 degrees applied sweep are shown. The disconnect between each of the four equations creates an issue when it comes to designing an aircraft with swept wings. The difference in the Critical Pressure Coefficient is the difference between designing a wing that meets the cruise performance targets versus missing crucial speed and fuel burn requirements.

Recall from our discussion that there is considerable variation in published 2D critical pressure equations, and that Kirkman & Takahashi's studies found that only Eastman Jacobs and Küchemann's equations [12],[20] were accurately predictors of incipient sonic flow.

For this study, we only seriously consider the Küchemann [12] and Eastman Jacobs [20] with the Neumark Modification [19], as potentially viable legacy predictive methods. Küchemann's equation, previously shown is: $Cp^* = \frac{2}{\gamma M_\infty^2}\left\{\left(\frac{2}{\gamma+1}\right)^{\frac{\gamma}{\gamma-1}}\left(1+\frac{\gamma-1}{2}M_\infty^2\,(\cos\varphi)^2\right)^{\frac{\gamma}{\gamma-1}}-1\right\}$, whereas Eastman Jacobs' modified by Neumark is: $Cp^* = \frac{2\left[1-\left(\frac{2+(\gamma-1)M_\infty^2(\cos\varphi)^2}{\gamma+1}\right)^{\gamma/(\gamma-1)}\right]}{\gamma M_\infty^2(\cos\varphi)^2}$.

These two equations have very different sweep transformations. Although they are equivalent for an unswept section, they vary vastly with the sweep corrections. In these equations, Küchemann transforms the pressure with the square of the cosine in the numerator only. Eastman Jacobs with the Neumark Modification shows the transformation with the square of the cosine in both the numerator and denominator.

The differences between the equations by Küchemann [12] and Eastman Jacobs [20] is shown in Figure 13 for a sweep angle of 40 degrees. At this sweep angle, the difference is very noticeable, and the same pressure coefficient could mean a critical Mach number around $M_\infty = 0.7$ or $M_\infty = 0.9$ depending upon which equation is correct.

The first sweep calculations were done ranging the Mach number from 0.6 to 0.9 by increments of 0.1. Figure 14 displays the results of the early runs. The shock wave begins to form at $M_\infty = 0.8$ and can be seen strengthening in the $M_\infty = 0.9$ solution. This is an early indicator to Küchemann's derivation being correct. In order to verify these solutions, further refinement was done around $M_\infty = 0.7$.

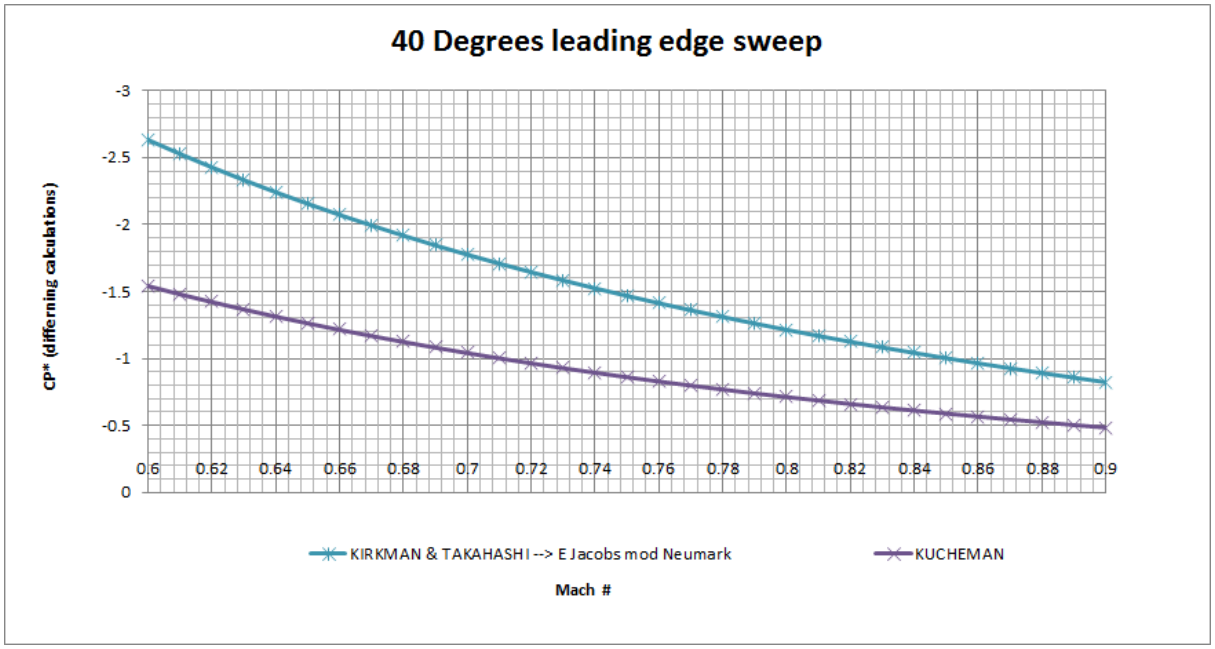

Figure 13. Comparision of Küchemann and Eastman Jacobs, with the Neumark Modification, Cp* equations used to predict the critical pressure coefficient of a wing with 40 degrees of sweep.

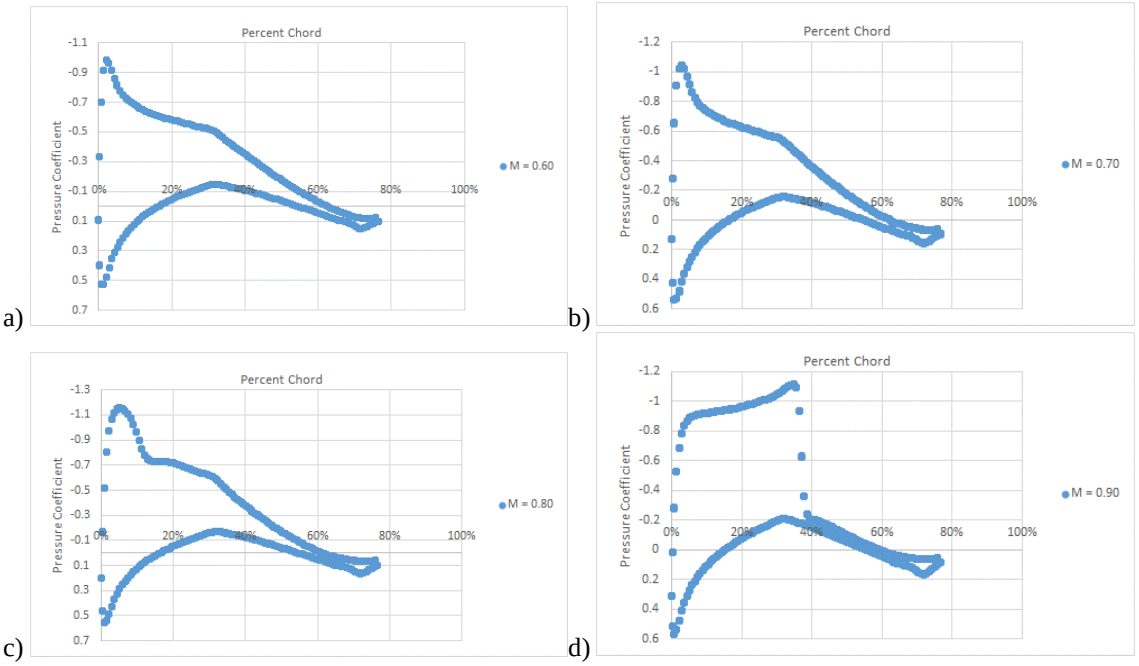

Figure 14. Coefficient of Pressure data from early trades on 40 degree swept airfoil section at 4 degrees angle of attack.

To confirm which equation is correct, the next ANSYS Fluent runs were performed on $M_\infty = 0.72$ with 40 degrees of sweep. At this flight condition, a shock wave is evident. This categorically indicates that Eastman Jacobs with Neumark Modification is incorrect. Figure 15 plots the pressure coefficient from the $M_\infty = 0.72$ run along with the critical pressure coefficient values from Küchemann and Eastman Jacobs with the Neumark modification. In this data it is evident that Küchemann correctly predicts the shock formation.

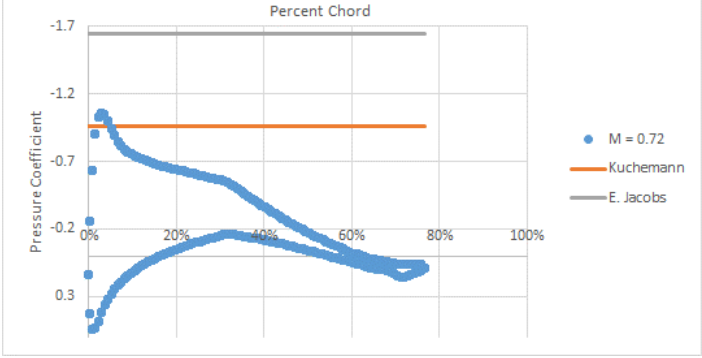

Figure 15. $M_\infty = 0.72$ data on NACA 64-012 airfoil section with 40 degrees sweep run at 4 degrees angle of attack.

To further confirm the accuracy of Küchemann [12], the model was reexamined at $M_\infty = 0.7$.

Figure 16 shows the data from the $M_\infty = 0.7$ run, where a shock wave is just beginning to form (as is evident from the pressure spike at the leading edge). This figure also plots the critical pressure coefficient value from Küchemann [12] and Eastman Jacobs [20] with the Neumark Modification [19].

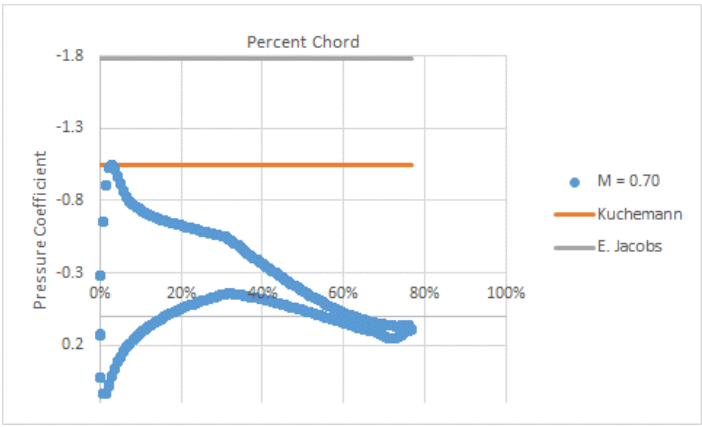

Figure 16. $M_\infty = 0.70$ data on NACA 64-012 airfoil section with 40 degrees sweep run at 4 degrees angle of attack.

In further refinement of this data, a grid convergence was attempted on the $M_\infty = 0.7$ data, however due to limitations on the computational memory, the grid was refined with a step size factor of 1.34. There were three grids in total, and the results of the grid refinement are shown in Table 1. The step size, *h*, is normalized to the coarsest grid.

Table 1 shows that the computational data output by ANSYS Fluent does not gain our ultimate confidence. Although the convergence is slow, the data does indeed show convergence with ever finer grids. For the purpose of this work, we used the pressure and velocity results arising from our coarse grid solutions.

Table 1. Results of the grid refinement performed on the swept airfoil test sections.

Step Size (h)	**Minimum Pressure (Cp_{min})**	**Maximum Mach**
1	-1.270	1.104
1.34	-1.1569	1.0374
1.80	-1.0434	0.9701
Richardson Extrapolation	-40.05	8.093
Observed Order (p)	0.00995	0.2439
GCI_{12} (Error Bar)	3817%	791%
GCI_{23} (Error Bar)	4203%	850%
Asymptote	0.91092	0.93966

Table 1 shows the importance of this element of our research. Although commercial CFD tools seem a compelling tool for validation, there are many steps that must be taken in order to confirm the resultant data is indeed correct. In this work properly modelling three-dimensional near sonic flows with a fine volume grid requires a significant

amount of available memory despite the seemingly simple geometry. In order to properly converge and verify the three-dimensional data, access to a large computing cluster is required for the necessary memory and computational power.

Our CFD data does indicate that Küchemann is correct in his derivation of the Critical Pressure Coefficient.

To understand further the physics behind Küchemann's derivation, we revisited his explanations in The Aerodynamic Design of Aircraft.

Küchemann derives the Critical Pressure Coefficient for a swept wing in Chapter 4 of his book. To begin he defines the local sonic condition for a swept wing: $(\frac{V}{V_0})^* = \{1 + \frac{2}{(\gamma+1)M_\infty^2}(1 - M_\infty^2 (\cos\varphi)^2\}^{\frac{1}{2}}$ which involves the local speed of sound (adjusted for pressure-temperature effects) which is: $a^2 = a_0^2 - \frac{1}{2}(\gamma - 1)(V_x^2 + V_y^2 + V_z^2 - V_0^2)$.

Simple sweep theory overlooks the compressibility effects of leading-edge as opposed to freestream reference frame pressure changes. Unlike the simple, geometric analogies given by Jones [6,10] or McLean[21] Küchemann, estimates the local speed of sound based upon pressure changes imposed by all of the perturbation velocities – both those in the leading edge reference frame and the cross flow reference frame. The total perturbation velocity is shown in the second portion of this equation as: $(V_x^2 + V_y^2 + V_z^2 - V_0^2)$. This shows that the higher the perturbation velocity, the lower the local speed of sound.

Küchemann's derivation is based upon the flow being homenergic (flow in which the sum of the kinetic energy, potential energy, and enthalpy per unit mass is the same at all locations and at all time in the fluid flow) [25] and isentropic, therefore this flow does not account for shock waves. This equation remains valid up until a shock wave occurs in the flow, which will not occur before the local flow exceeds the sonic point.

In order to transform with the proper sweep equation Küchemann derives the equation of motion based upon the transformations found in equations 19a through 19c and 20a through 20c.

$$\xi = x\cos\varphi - y\sin\varphi \quad (19a)$$
$$\eta = x\sin\varphi + y\cos\varphi \quad (19b)$$
$$\zeta = z \quad (19c)$$
$$V_{\xi 0} = V_0\cos\varphi\cos\alpha \quad (20a)$$
$$V_{\eta 0} = V_0\sin\varphi\cos\alpha \quad (20b)$$
$$V_{\zeta 0} = V_0\sin\alpha \quad (20c)$$

These transformations can be viewed as figure 17. This figure shows the sketches made by Küchemann and the transformations he makes for the swept wing.

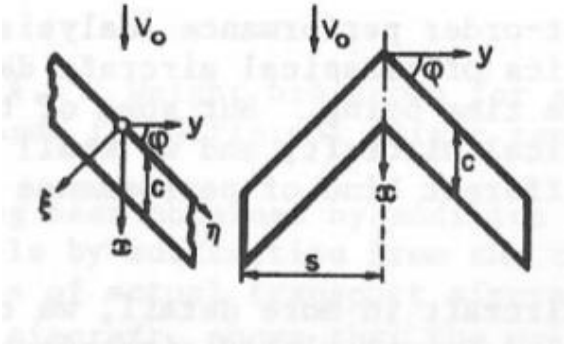

Figure 17. Küchemann's sketch on the coordinate transformation for swept wings.

Küchemann does not dispute the claims that the sonic conditions are based upon the flow normal to the leading edge. Instead, he continues to support this claim. Küchemann argues that critical conditions are based upon the flow normal to the leading edge, yet the local speed of sound is still dependent upon the perturbations of the entire flow. It is an interesting claim that Küchemann makes, and one that is similar to the explanation of oblique shock properties from NACA TM- 1135 [22].

Küchemann's [12] derivation of the flow around a swept wing is reproduced here as equations 21 through 25. He states that the flow is governed by:

$$1 - \frac{(\partial\Phi/\partial\xi)^2 + (\partial\Phi/\partial z)^2}{a^2} = 0 \quad (21)$$

Where a^2 is the local speed of sound squared and:

$$\frac{\partial\Phi}{\partial\xi} = V_\xi = V_0 \cos\varphi \cos\alpha + v_\xi \quad (22)$$

$$\frac{\partial\Phi}{\partial z} = V_z = V_0 \sin\alpha + v_z \quad (23)$$

In these equations, V_0 is the freestream flow velocity, φ is the sweep angle, α is the angle of attack, and v_ξ and v_z are the perturbation velocities in the ξ and z directions respectively. Therefore, rearranging equation 21 and plugging in 22 for $\partial\Phi/\partial\xi$ and 23 for $\partial\Phi/\partial z$, the equation becomes:

$$V_\xi^2 + V_z^2 = a^2 = V_n^2 \quad (24)$$

Or:

$$V^2 - V_\eta^2 = V_0^2(\sin\varphi)^2\,(\cos\alpha)^2 = a^2 \quad (25)$$

Küchemann indicates the velocity that determines the critical condition is the velocity normal to the leading edge of the wing, whereas the total velocity of the flow could indeed exceed the sonic point. This is shown by equation 23, where the total velocity is shown as, *V*, and the freestream velocity as, V_0.

Küchemann's final derivation of the Critical Pressure Coefficient fundamentally differs from the explanations of Busemann [2] and Jones [6]. In this scenario, Küchemann shows that the Mach number normal to the leading edge does indeed matter, yet this is not the only consideration. With Küchemann's derivations, it is evident he includes the perturbation velocities into his equation and considers a change in the local speed of sound to the flow. This derivation mimics results found in the CFD data gathered.

V. Conclusions

While the ANSYS Fluent solutions for the swept sections do not provide complete confidence, our grid refinement study indicates shows that the data does indeed converge, albeit slowly. Although it is not ideal, the grid refinements were showing the expected trend in the data, which showed the shock wave strengthening with the finer grid resolutions. In order to further verify this data, further grid refinements must be completed on systems with improved computing power. The data must be built and run on a much finer grid and confirmed with the results presented here to ensure true convergence of the CFD data.

The data presented from the swept wing sections show that Küchemann's derivation is indeed correct. Küchemann postulated that the Critical Pressure Coefficient depends upon both the freestream Mach number and the Mach number normal to the leading edge. This is conceptually similar to Schlichting's approach but fundamentally differs from the work of Neumark or Jones. Küchemann does not dispute the claim that the flow normal to the leading edge must exceed the sonic condition, however he does argue that the sonic condition is a function of the total perturbation velocity from the freestream. Therefore, the freestream Mach number still has importance in determining the Critical Pressure Coefficient.

The differences between the Küchemann equation and other implementations of simple sweep theory are not trival. For a 40-degree swept wing the difference in predicted as opposed to actual critical pressure coefficient may vary by as much as 100% (refer back to Figures 13, 15 and 16). Thus, a wing designed using simple sweep theory rules could easily miss its critical Mach number target by speeds as great as $\Delta M=0.1$.

We believe that Küchemann's equation effectively predicts incipient sonic flow. The incorporation of this method into the potential flow based wing design process enables the development of new rapid physics based geometric synthesis tools..

Acknowledgements

This paper derives from unsponsored research performed by Mr. Kirkman in partial fulfillment of the requirements for the degree of Master of Science in Aerospace Engineering at Arizona State University.

References

1. Gabrielli, G. and von Karman, T., "What price speed? Specific power required for propulsion of vehicles", *Mechanical Engineering* **72** (1950), #10, pp. 775-781.
2. Busemann, A. (1935). *Aerodynamischer Auftrieb bei Überschallgeschwindigkeit.* Luftfahrtforschung Vol. 12, No. 6, 1935, pp. 210-215.
3. Meier, H. (Ed.). (2010). Chapter 1: Historic Review of the Development of High-Speed Aerodynamics (E. Stanewsky, Trans.). In *German Development of the Swept Wing* (pp. 1-68). American Institute of Aeronautics and Astronautics.
4. Meier, H. (Ed.). (2010). Chapter 2: High Speed Flight and Its Aerodynamic and Gas Dyanmic Challenges. In *German Development of the Swept Wing* (pp. 69-269). American Institute of Aeronautics and Astronautics.
5. Ackeret, J., Degen, M. & Rott N. (1951) *Investigations on Wings with and without Sweepback at High Subsonic Speeds*. (National Advisory Committee for Aeronautics TM 1320).
6. Jones, Robert T. (1945) *Wing Plan Forms for High-Speed Flight* (National Advisory Committee for Aeronautics TR 863).
7. Takahashi, T. T., Dulin, D. J., & Kady, C. T. (2014). *A Method to Allocate Camber, Thickness and Incidence on a Swept Wing.* (American Institute of Aeronautics and Astronautics). AIAA 2014-3172.
8. Takahashi, T. T., & Kamat, S. (2015). *Revisiting Busemann: The Design Implications of Inconsistencies Found Within Simple Sweep Theory*. (American Institute of Aeronautics and Astronautics). AIAA 2015-3376.
9. Kirkman, J. J. & Takahashi, T.T. (2016). *Revisiting the Transonic Similarity Rule: Critical Mach Number Prediction Using Potential Flow Solutions*. (American Institute of Aeronautics and Astronautics). AIAA 2016
10. Jones, R. T., & Cohen, D. (1960). *High speed wing theory*. Princeton, NJ: Princeton University Press.
11. Anderson, J. (2005). 5.9 Critical Mach Number and Critical Pressure Coefficient. In *Introduction to Flight* (Fifth ed., pp. 283-294). New York, NY: McGraw Hill.
12. Küchemann, D. (2012). *The Aerodynamic Design of Aircraft* (AIAA Education Series). Reston, VA: American Institute of Aeronautics and Astronautics.
13. Bertin, J. J., & Cummings, R. M. (2014). 9.4 Swept Wing at Transonic Speeds. In *Aerodynamics for Engineers* (Sixth ed., pp. 527-543). Pearson.
14. Schlichting, H., & Truckenbrodt, E. (1979). Aerodynamics of the Airplane (H. J. Ramm, Trans.). McGraw-Hill.
15. Ludweig, H., Verringerung des Widerstandes von Traglugeln bei hohen Geschwindingkeiten durch Pfeilform., AVA 39/H/18, Wiss 8, Dec 29, 1939.
16. Ackeret, J., Degen, M. & Rott N. (1951) *Investigations on Wings with and without Sweepback at High Subsonic Speeds*. (National Advisory Committee for Aeronautics TM 1320).
17. Betz, A. "Applied Airfoil Theory. Unsymmetrical and Non-Steady Types of Motion" In *Aerodynamic Theory*, div. J, ch. IV, sec. 2, W. F. Durand, cd., Juiius Springer (Berlin), 1935, pp. 97-99.
18. Miranda, L. R., Baker, R. D., & Elliott, W. M., (1977) *A Generalized Vortex Lattice Method for Subsonic and Supersonic Flow* NASA CR 2875.
19. Neumark, S. (1949). *Critical Mach Numbers for Thin Untapered Swept Wings at Zero Incidence*. (Aeronautical Research Council Reports and Memoranda No. 2821).
20. Von Kármán, T. (1941). Compressibility Effects in Aerodynamics. *Journal of the Aeronautical Sciences, 8*(9), 337-355.
21. McLean, D. (2013). 7.4.8 Airfoils in Transonic Flow. In *Understanding Aerodynamics* (pp. 342-350). John Wiley & Sons.
22. *Equations, Tables, and Charts for Compressible Flow*. (National Advisory Committee for Aeronautics Report 1135).

23. Milne-Thomson, L. M. (1973). 16.4 Shock Waves. In *Theoretical Aerodynamics* (pp. 302-304). NY: Dover Publications.
24. SAS IP, Inc., *Section 20.1.2. Density-Based Solver*, The ANSYS Fluent Getting Started Guide, Release 15.0
25. Homenergic Flow. (n.d.). Retrieved March 25, 2016, from http://encyclopedia2.thefreedictionary.com/homenergic flow